Hindawi
Shock and Vibration
Volume 2023, Article ID 5827471, 11 pages
https://doi.org/10.1155/2023/5827471

Research Article

The Seismic Design Process of RC Column Components in SDOF System considering the Earthquake Duration Effect

Yukui Wang[1,2] **Dan Zhang**,[1,3] **Jing Liu**,[1,3] **Zhangqi Hu**[1,3] **and Dou Zhong**[1]

[1]*College of Civil Engineering, Hunan City University, Yiyang 413099, China*
[2]*Key Laboratory of Green Building and Intelligent Construction in Higher Educational Institutions of Hunan Province, Hunan City University, Yiyang 413000, China*
[3]*Hunan Engineering Research Center of Development and Application of Ceramsite Concrete Technology, Hunan City University, Yiyang 413099, China*

Correspondence should be addressed to Yukui Wang; 1219464373@qq.com

Received 25 April 2023; Revised 21 June 2023; Accepted 27 July 2023; Published 7 August 2023

Academic Editor: Roberto Nascimbene

In order to study seismic design process of RC (reinforced concrete) column components considering the effect of earthquake duration, the degradation law of capacity under random amplitude hysteresis history was conducted by the research group, and the estimation method for the energy dissipation capacity of RC column components was suggested. Furthermore, the correlation between the stiffness decay index and energy dissipation capacity, hysteresis histories, and structural parameters was proposed, and the performance classification criteria based on the stiffness decay index was established. On this basis, the connection between the stiffness decay index and structural parameters and seismic parameters was established, and the seismic design process of RC column components in SDOF (single degree of freedom) system was proposed. The research indicated that the proposed seismic design process based on stiffness decay index can effectively consider the effect of earthquake duration. The stiffness decay index is more suitable for defining structural damage than deformation index and Park-Ang index. The stiffness decay index establishes quantitative relationships with seismic parameters and structural parameters, facilitating performance-based design in engineering practice. The increase in earthquake duration exacerbates the damage of RC column components, and this effect is more pronounced at the beginning of the earthquake and gradually decreases over time.

1. Introduction

The maximum amplitude deformation experienced by structures under seismic action and the earthquake duration are two important factors that contribute to structural damage [1–5]. The earthquakes in Fukushima, Japan (2011), Chile (2010), and Wenchuan, China (2008), lasted for the durations of 300 seconds, 200 seconds, and 180 seconds, respectively. Long-duration ground motion period often causes severe damage to structures [6, 7]. However, the current seismic design methods do not sufficiently consider the effect of earthquake duration [8]. Therefore, it is essential to study the effect of earthquake duration when developing a performance-based seismic design method.

To study the duration effect of earthquakes, it is first necessary to understand the impact of variable amplitude hysteresis loading paths on the capacity degradation [9]. Previous studies have shown that there is no significant relationship between the earthquake duration and the maximum amplitude deformation [10–12]. However, a strong correlation has been observed between the cumulative hysteresis energy dissipation and the earthquake duration [13–16]. As a result, the cumulative hysteresis energy dissipation is widely accepted as an effective measure to describe the impact of earthquake duration [17, 18]. Scholars have extensively studied the cumulative hysteresis energy dissipation of RC structures. Goodnight et al. [9] have discovered that the sequence of maximum amplitude deformation within the hysteresis history has a significant

impact on the cumulative hysteresis energy dissipation. While Poljanšek et al. [19] have carried out statistical analysis on the ultimate deformation capacity of RC column components, they have not considered the impact of hysteresis history on the ultimate deformation capacity. Yuan and Wang [20] have observed that the degradation of energy dissipation capacity becomes more severe as the maximum amplitude deformation occurs earlier in the hysteresis history. Erberik and Sucuoğlu [13, 14] have found that the residual energy dissipation capacity under variable amplitude hysteresis history is not only associated with the cumulative hysteresis energy dissipation but also with the specific characteristics of the variable amplitude hysteresis history. Jiao et al. [21] investigated the influence of different loading histories on the deformation capacity and energy dissipation capacity of steel beams and proposed an evaluation method of energy dissipation capacity. However, the conclusions lack sufficient guidance for reinforced concrete components.

In order to study seismic design process of RC column components considering the effect of earthquake duration, the degradation law of capacity under random amplitude hysteresis history was studied by the research group, and the estimation method for the energy dissipation capacity of RC column components was proposed [22, 23]. Furthermore, the correlation between the stiffness decay index and energy dissipation capacity, hysteresis histories, and structural parameters was established [24]. On this basis, the relationship between stiffness decay index and both structural parameters and seismic parameters was established, and the seismic design process of RC column components was proposed. This seismic design method can make up for the lack of considering the duration effect in current seismic design codes.

2. Stiffness Decay Index

2.1. Equation for Stiffness Decay Index. Figure 1 shows the loading stiffness K_k of the k-th half hysteresis. The ratio of loading stiffness to initial loading stiffness is defined as the stiffness decay index, which can reflect the damage state of the column components at each half hysteresis. The stiffness decay index can be obtained from the following equation:

$$D_{K,k} = 1 - \frac{K_k}{F_y/\Delta_y}. \tag{1}$$

Here, F_y is the yield force and Δ_y is the yield displacement.

The stiffness decay law of RC column components under variable amplitude hysteresis history was studied by the research group, and the correlation between the stiffness decay index and energy dissipation capacity, hysteresis histories, and structural parameters was explored. Based on this, the estimation method of stiffness decay index was proposed [24].

$$D_{\mathrm{K},k} = \left(A_{\max}\left(1 - e^{-B_{\max}\left(n_k - 0.64n_{1,\max} + 3.57\right)}\right)\right)^4, \tag{2}$$

with

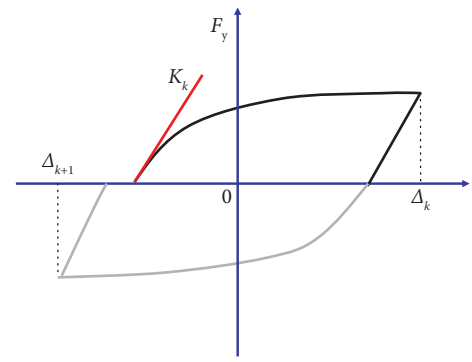

Figure 1: The loading stiffness K_k of the k-th half hysteresis.

$$A_{\max} = 0.94\left(1 - \left(0.42 - 0.38e^{-355\rho_{\mathrm{sr}}}\right)^{u_{k,\max}}\right), \tag{3}$$

$$B_{\max} = \frac{7.72e^{0.22-200\rho_{\mathrm{sr}}} - 0.22}{\left(1 + u_{k,\max}\right)^{2.3-96\rho_{\mathrm{sr}}}}, \tag{4}$$

$$u_{k,\max} = \frac{\Delta_{k,\max}}{\Delta_y}, \tag{5}$$

$$n_k = \frac{\sum_{i=1}^{k} E_{H,i}}{0.5F_y\Delta_y}. \tag{6}$$

Here, $A_{\max}$ represents the severity of damage for RC column components, $B_{\max}$ represents the speed of damage development for RC column components, n_k is the nominal cumulative hysteresis energy from the 1st to the k-th half hysteresis, $n_{1,\max}$ is the nominal cumulative hysteresis energy of the 1st half hysteresis at subsequent large displacement amplitude stage, $u_{k,\max}$ is the maximum nominal displacement in the hysteresis history, $\Delta_{k,\max}$ is the maximum displacement in the hysteresis history, ρ_{sr} is the transverse reinforcement ratio of the RC column components, and $\sum_{i=1}^{k} E_{\mathrm{H},i}$ is cumulative hysteresis energy from the 1st to the k-th half hysteresis.

The estimation method of stiffness decay index $D_{K,k}$ can be obtained from equations (2)–(6) as follows:

$$D_{K,k} = f\left(\rho_{\mathrm{sr}}, F_y, \Delta_y, \Delta_{k,\max}, \sum_{i=1}^{k} E_{H,i}\right). \tag{7}$$

From equation (7), it can be seen that the stiffness decay index $D_{K,k}$ is effectively related to the structural parameters (F_y, Δ_y, and ρ_{sr}), hysteresis history ($\Delta_{k,\max}$), and cumulative hysteresis energy ($\sum_{i=1}^{k} E_{H,i}$).

2.2. Performance Classification Criteria Based on Stiffness Decay Index [24]. Previous research has found that the stiffness decay index $D_{K,k}$ can be used to classify the performance criteria of RC column components [24]. The stiffness decay index $D_{K,k}$ less than 0 indicates the undamaged stage, where no visible cracks are present on the concrete surface of the RC column components. The stiffness decay index $D_{K,k}$ between 0 and 0.4 indicates the mild

damage stage, and the corresponding damage phenomenon is that multiple horizontal cracks appear on the concrete surface (with crack widths ranging from 0.03 mm to 0.08 mm). The stiffness decay index $D_{K,k}$ between 0.4 and 0.6 indicates the moderate damage stage, where the early cracks continue to develop and start to connect end-to-end (with crack widths ranging from 0.08 mm to 0.21 mm). The stiffness decay index $D_{K,k}$ between 0.6 and 0.8 indicates the severe damage stage, where the horizontal cracks from the early stage transform into unidirectional oblique cracks (with crack widths ranging from 0.21 mm to 1.35 mm), and with the further development of damage, these unidirectional oblique cracks develop into intersecting cracks (with crack widths ranging from 1.35 mm to 3.2 mm), resulting in severe spalling on the surface of the concrete. At this stage, the RC column components lose their repairable value. The stiffness decay index $D_{K,k}$ between 0.8 and 1 indicates the destructive stage, where the concrete in the core area of the RC column components is crushed. Figure 2 shows the damage phenomenon of the specimen. Table 1 shows the performance classification criteria based on the stiffness decay index $D_{K,k}$.

3. The Correlations of Stiffness Decay Index with Deformation Index and Park-Ang Index

The correlations of stiffness decay index with deformation index and Park-Ang index are discussed by using the test data of 9 specimens [23]. The reinforcement parameters and loading hysteresis histories of the 9 specimens are shown in Table 2. Four hysteresis histories are used, numbered as S1, S1-S, S1-L, and S2. Figure 3 shows four types of loading hysteresis histories. See [23] for more details on the test.

3.1. The Correlation between Stiffness Decay Index and Deformation Index. The deformation index D_{drift} of RC column components can be calculated by the following equation:

$$D_{\text{drift}} = \frac{\Delta_{k,\max}}{H}. \tag{8}$$

Here, H represents the height of RC column components.

Figure 4(a) shows the correlation between the stiffness decay index $D_{K,k}$ and the deformation index D_{drift}, indicating a positive correlation relationship between the two. In the range of $0 < D_{K,k} \le 0.4$ (and $0 < D_{\text{drift}} \le 0.006$), $D_{K,k}$-D_{drift} relations show an approximate linear growth pattern, but after $D_{K,k} > 0.4$ (and $D_{\text{drift}} > 0.006$), the dispersion of data points significantly increases. According to the performance classification criteria of the stiffness decay index, it can be observed that when $0 < D_{K,k} \le 0.4$, it corresponds to the stage of mild damage. When $0.4 < D_{K,k} \le 0.6$, it corresponds to the stage of moderate damage. Also, when $0.6 < D_{K,k} \le 0.8$, it corresponds to the stage of severe damage. Therefore, it can be concluded that the stiffness decay index and the deformation index have a good correspondence in describing mild damage. However, they have not established a corresponding relationship in describing moderate and severe damage.

Figure 4(b) shows the effect of reinforcement conditions on $D_{K,k}$-D_{drift} relations. By comparing the $D_{K,k}$-D_{drift} relation of specimens R1 and R7, it can be found that under the identical hysteresis history, the reinforcement conditions result in a clear stratification of the $D_{K,k}$-D_{drift} relations. The $D_{K,k}$-D_{drift} relation of specimen R7 with relatively more reinforcement is below the $D_{K,k}$-D_{drift} relation of specimen R1 with relatively less reinforcement. A similar phenomenon can be obtained by comparing the $D_{K,k}$-D_{drift} relation of specimens R2 and R8. This indicates that when the stiffness decay index $D_{K,k}$ remains unchanged, the increase in reinforcement enables the RC column components to withstand larger deformation.

Figure 4(c) shows the effect of hysteresis histories on the $D_{K,k}$-D_{drift} relations. By comparing the $D_{K,k}$-D_{drift} relation of specimens R4 to R6, it can be found that under the identical reinforcement condition, the hysteresis histories result in a clear stratification of the $D_{K,k}$-D_{drift} relations. The $D_{K,k}$-D_{drift} relation of specimen R4 (the maximum amplitude deformation occurs at the end of the hysteresis process) is located at the top, while the $D_{K,k}$-D_{drift} relation of specimen R6 (the maximum amplitude deformation occurs in the early stage of the hysteresis process) is located at the bottom. It can be seen that when the maximum amplitude deformation occurs in the early stage of the hysteresis process, the RC column components can bear large deformation with relatively small damage.

Figure 4(d) shows the effect of duration on $D_{K,k}$-D_{drift} relations. By comparing the $D_{K,k}$-D_{drift} relation of specimens R2 and R3, it can be found that under the identical reinforcement condition, the duration results in a clear stratification of the $D_{K,k}$-D_{drift} relations. The $D_{K,k}$-D_{drift} relation of specimen R3 (long-duration) is below the $D_{K,k}$-D_{drift} relation of specimen R2 (short-duration). A similar phenomenon can be obtained by comparing the $D_{K,k}$-D_{drift} relations of specimens R7 and R8. This indicates that when the stiffness decay index $D_{K,k}$ remains unchanged, the deformation capacity is reduced under the long-duration earthquake action.

In summary, the stiffness decay index $D_{K,k}$ and deformation index D_{drift} have good correspondence in describing mild damage of RC column components. However, they have not established a corresponding relationship in describing moderate and severe damage. The reinforcement conditions, hysteresis histories, and earthquake duration have a significant impact on the $D_{K,k}$-D_{drift} relations.

3.2. The Correlation between Stiffness Decay Index and Park-Ang Index. The Park-Ang index $D_{\text{Park-Ang}}$ of RC column components can be calculated by the following equation [25]:

$$D_{\text{Park-Ang}} = \frac{x_m}{x_u} + \beta \frac{\sum_{i=1}^{k} E_{H,i}}{F_y x_u}. \tag{9}$$

Table 1: The performance classification criteria based on the stiffness decay index [24].

Nos.	Stiffness decay index $D_{K,k}$	Damage phenomenon	Damage stage	Performance criteria
1	$D_{K,k} < 0$	No visible cracks	No damage	Intact
2	$0 < D_{K,k} \leq 0.4$	Multiple horizontal cracks	Mild damage	Repairable
3	$0.4 < D_{K,k} \leq 0.6$	Horizontal cracks connecting end to end	Moderate damage	
4	$0.6 < D_{K,k} \leq 0.8$	Unidirectional oblique cracks, intersecting cracks	Severe damage	No collapse
5	$0.8 < D_{K,k} \leq 1$	Concrete crushed	Destruction	Collapse

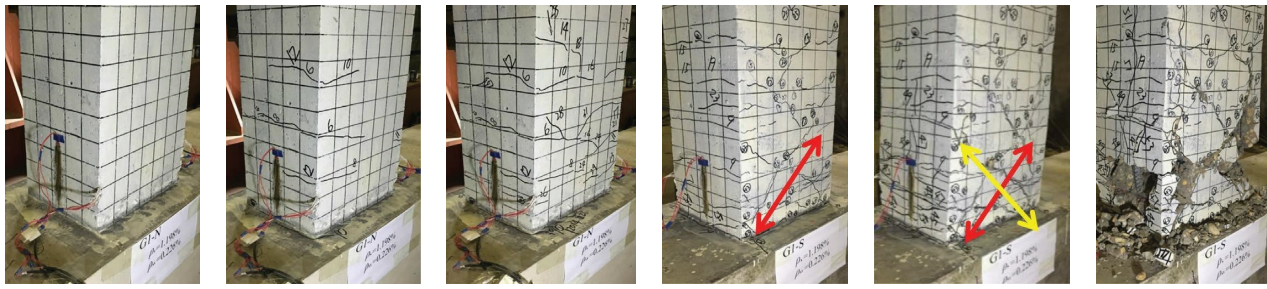

(a) (b) (c) (d) (e) (f)

Figure 2: The damage phenomenon of the specimen. (a) No visible cracks. (b) Multiple horizontal cracks. (c) Horizontal cracks connecting end to end. (d) Unidirectional oblique cracks. (e) Intersecting cracks. (f) Concrete crushed.

Table 2: The reinforcement parameters and loading hysteresis histories of the 9 specimens.

Nos.	Transverse reinforcement ratio ρ_{sr} (%)	Longitudinal reinforcement ratio ρ_r (%)	Hysteresis history	Number of half hysteresis cycles
R1	0.226	0.587	S1-S	42
R2	0.226	0.587	S1	42
R3	0.226	0.587	S2	178
R4	0.226	1.198	S1-S	42
R5	0.226	1.198	S1	42
R6	0.226	1.198	S1-L	42
R7	0.804	1.198	S1-S	42
R8	0.804	1.198	S1	42
R9	0.804	1.198	S2	178

Here, x_u is the ultimate deformation of the structure under monotonic loading, x_m is the maximum deformation of the structure under earthquake action, and β is the influence factor related to the shear span ratio, axial compression ratio, and reinforcement parameters [25].

The performance classification criteria based on the Park-Ang index was proposed [26]. According to the criteria, if the Park-Ang index is below 0.4, the structure can be repaired. However, if the Park-Ang index exceeds 1.0, the structure is considered to be in a state of destruction.

Figure 5(a) shows the correlation between the stiffness decay index $D_{K,k}$ and the Park-Ang index $D_{\text{Park-Ang}}$, indicating a positive correlation between the two. The upper and lower shadow areas in the Figure 5(a) are divided into destructive and nondestructive zones based on the performance criteria of stiffness decay index and Park-Ang damage index. The data points with $D_{\text{Park-Ang}} < 1.0$ are located in the green shaded area, indicating that using the Park-Ang index to define the nondestructive state of RC column components is consistent with using the stiffness decay index to define the nondestructive state. When $D_{\text{Park-Ang}} > 1$, some data points are located in the red shaded area, while others are located in the severe damage range defined by the stiffness decay index. This indicates that when defining the destructive behavior of RC column components, utilizing the stiffness decay index tends to yield less conservative results compared to the Park-Ang index.

Figures 5(b)–5(d) show the effects of reinforcement conditions, hysteresis histories, and earthquake duration on the $D_{K,k}$-$D_{\text{Park-Ang}}$ relations, respectively. The upper and lower shadow areas are divided into repairable and nonrepairable zones based on the performance criteria of stiffness decay index and Park-Ang index. It can be found that except for specimen R6 (where the maximum amplitude deformation occurs in the early stage of the hysteresis process) in Figure 5(c), most of the data points fall within the shaded areas. This indicates that the Park-Ang index shows good consistency with the stiffness decay index in evaluating the repairable state of RC column components, but when the maximum amplitude deformation occurs in the early stage

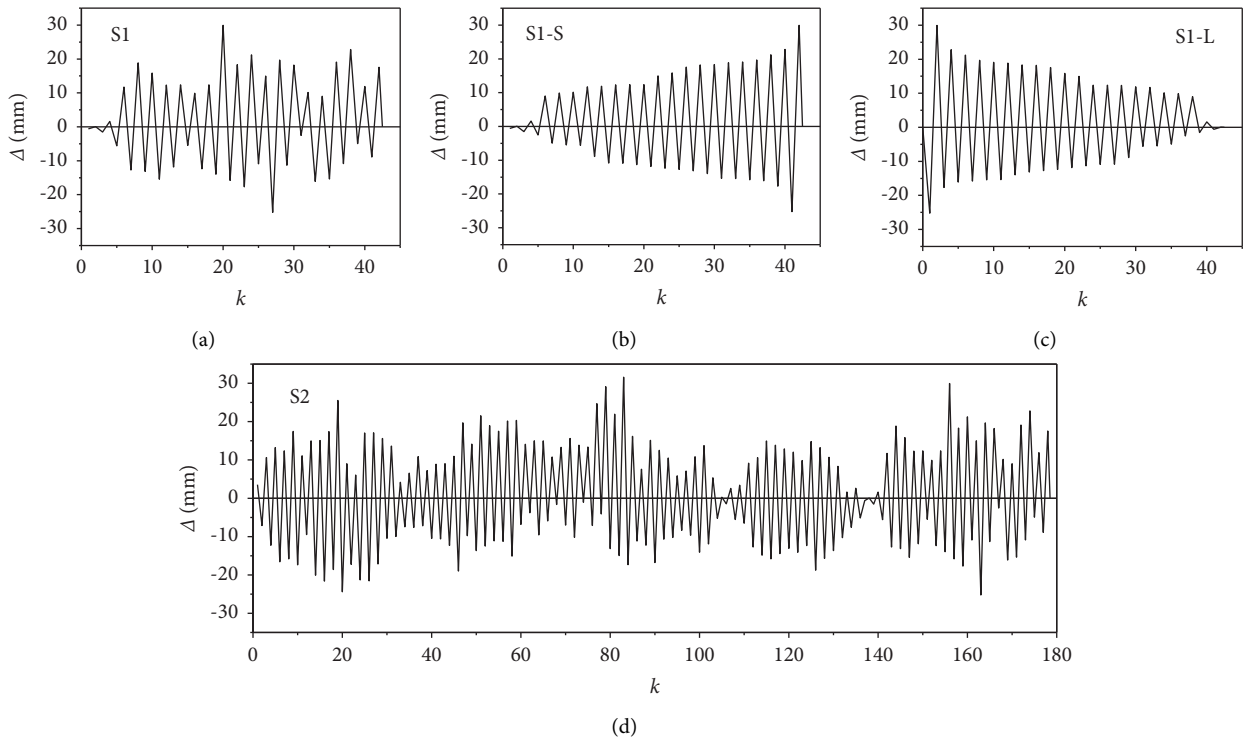

Figure 3: Four types of loading hysteresis histories [23]: (a) hysteresis history S1, (b) hysteresis history S1-S, (c) hysteresis history S1-L, and (d) hysteresis history S2.

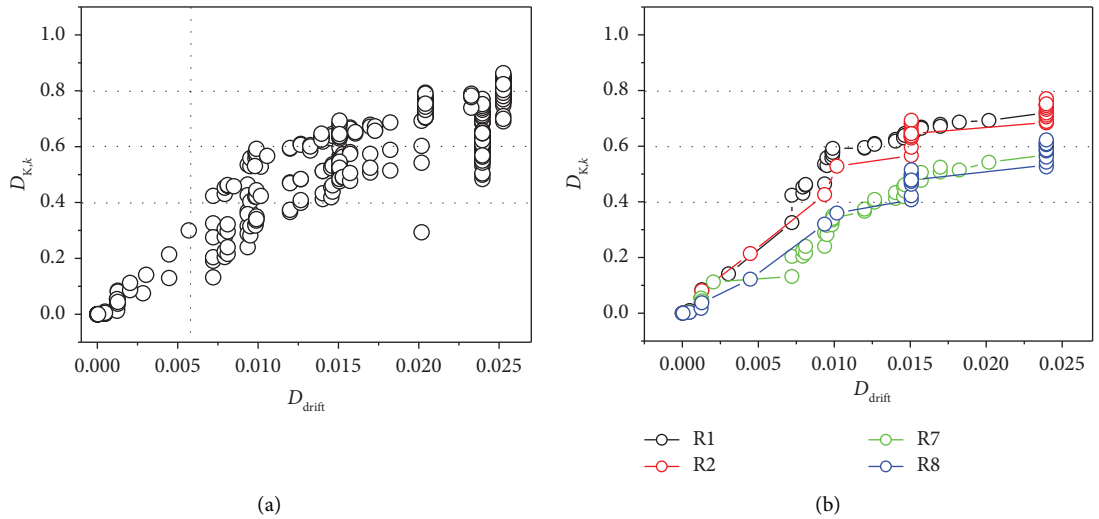

Figure 4: Continued.

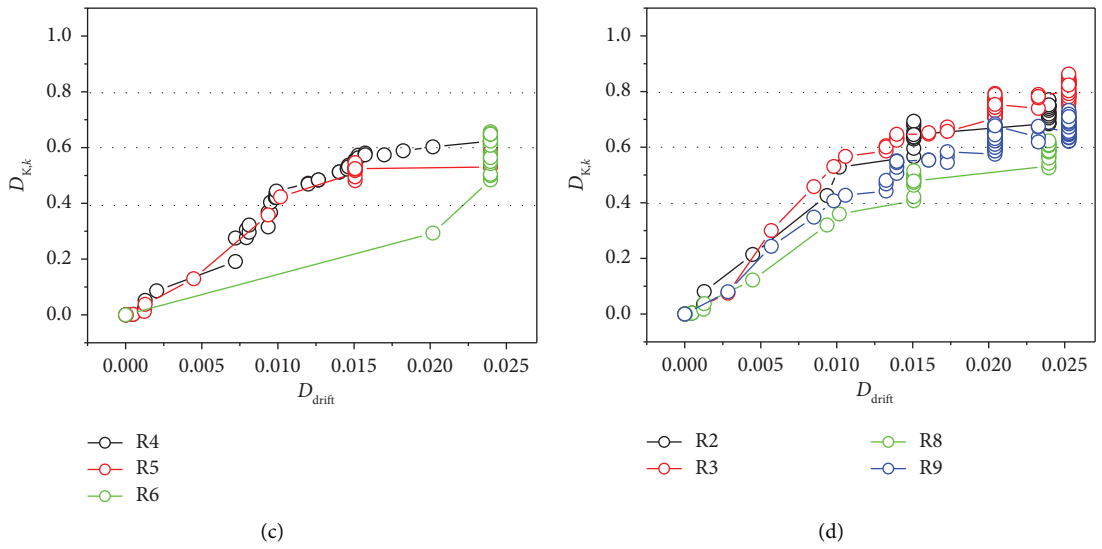

FIGURE 4: Effects of reinforcement conditions, hysteresis histories, and earthquake duration on the $D_{K,k}$-D_{drift} relations. (a) The correlation between $D_{K,k}$ and D_{drift}. (b) Effect of reinforcement conditions on $D_{K,k}$-D_{drift} relations. (c) Effect of hysteresis histories on $D_{K,k}$-D_{drift} relations. (d) Effect of duration on $D_{K,k}$-D_{drift} relations.

of the hysteresis history, the Park-Ang index tends to be more conservative in assessing the repairable state compared to the stiffness decay index.

By comparing the green shaded areas in Figures 5(b)–5(d), it can be found that the differences of reinforcement conditions, hysteresis histories, and earthquake duration result in a clear stratification of the $D_{K,k}$-$D_{\text{Park-Ang}}$ relations. This indicates a lack of consistency between the Park-Ang index and the stiffness decay index when evaluating mild and moderate stages of damage.

In summary, the stiffness decay index and Park-Ang index demonstrate good consistency in defining nondestructive and repairable states. However, they lack consistency when defining mild and moderate damage states.

4. Seismic Design Process Based on Stiffness Decay Index

4.1. The Correlation between Stiffness Decay Index and Seismic Parameters. From equation (7), it can be seen that the stiffness decay index $D_{K,k}$ is effectively related to the structural parameters, hysteresis histories, and cumulative hysteresis energy. In order to determine the correlation between stiffness decay index $D_{K,k}$ and seismic parameters, the cumulative hysteresis energy $\sum_{i=1}^{k} E_{H,i}$ for the SDOF system can be calculated by the following equation [17]:

$$\sum_{i=1}^{k} E_{H,i} = m\phi E_1, \tag{10}$$

with

$$\phi = 1.13\frac{(\mu-1)^{0.82}}{\mu}, \tag{11}$$

$$E_1 = 0.5\left(\eta V_g\right)^2, \tag{12}$$

$$\eta = \begin{cases} \eta^*\left(\dfrac{2T}{T_g} - \left(\dfrac{T}{T_g}\right)^2\right) T < T_g, \\ \eta^*\left(\dfrac{T}{T_g}\right)^{-\lambda} T > T_g, \end{cases} \tag{13}$$

$$T_g = 2\pi\frac{\nu_1 V_g}{\nu_2 A_g}, \tag{14}$$

$$\eta^* = \frac{0.25A_g}{V_g}\sqrt{t_d T_g}\sqrt{\frac{\lambda+0.5}{2\lambda+2}}. \tag{15}$$

Here, m represents the mass of the structure, φ represents the proportional parameter, E_1 represents the seismic input energy, V_g and A_g represent the peak value of ground velocity and peak value of ground acceleration, respectively, η is the amplification coefficient of peak ground velocity, η^* is the amplification coefficient of the seismic input energy, λ is the site type parameter, T represents the fundamental period, T_g represents the characteristic period of the site, ν_1 is the ratio of elastic response velocity to peak ground velocity, ν_2 is the ratio of elastic response acceleration to peak ground acceleration, the coefficients ν_1 and ν_2 were taken as 1.9 and 2.4, respectively [27], and t_d is the earthquake duration.

According to equations (10)–(15), the stiffness decay index $D_{K,k}$ can be obtained as follows:

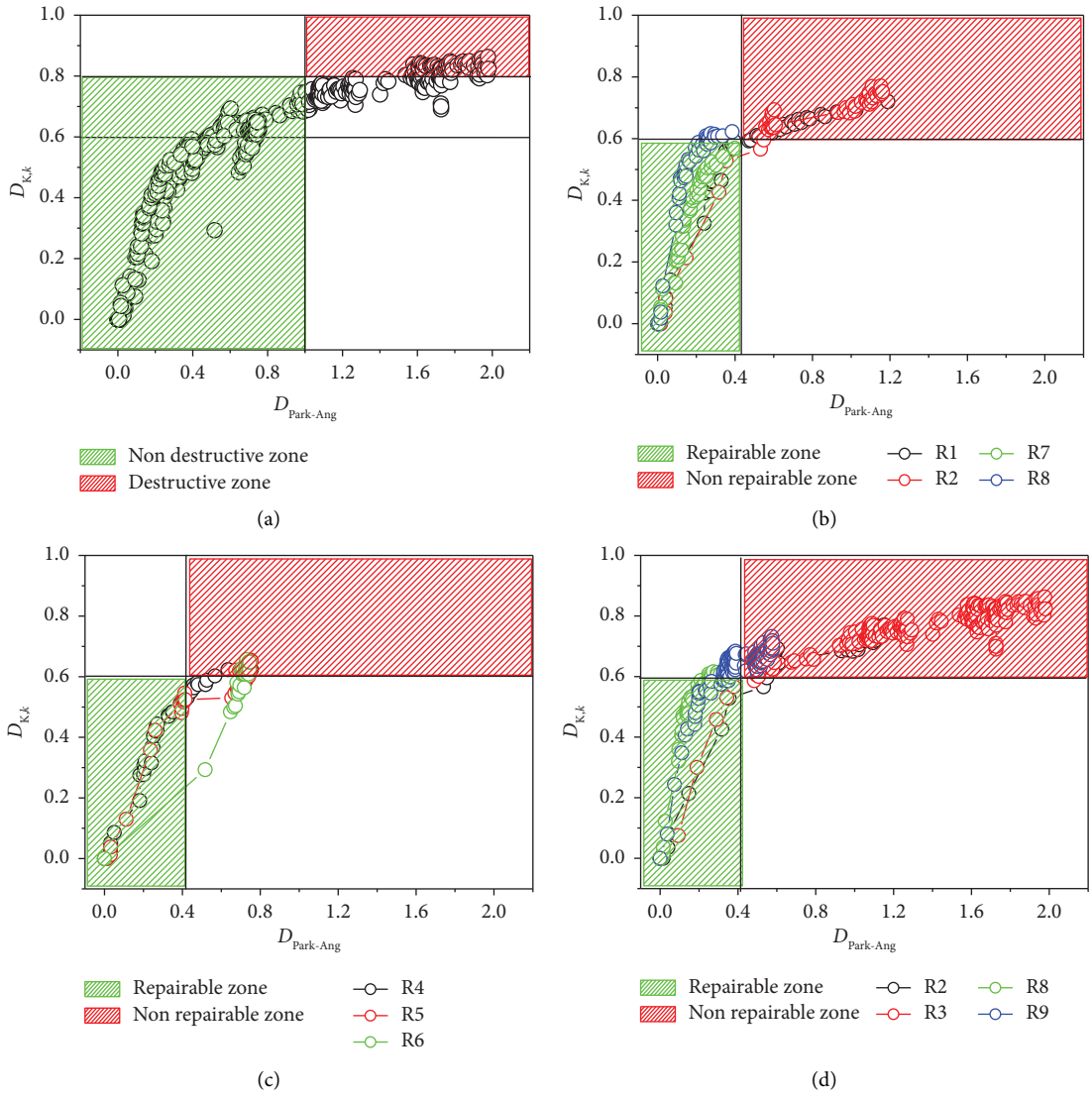

FIGURE 5: Effects of reinforcement conditions, hysteresis histories, and earthquake duration on the $D_{K,k}$-$D_{\text{Park-Ang}}$ relations. (a) The correlation between $D_{K,k}$ and $D_{\text{Park-Ang}}$. (b) Effect of reinforcement conditions on $D_{K,k}$-$D_{\text{Park-Ang}}$ relations. (c) Effect of hysteresis histories on $D_{K,k}$-$D_{\text{Park-Ang}}$ relations. (d) Effect of duration on $D_{K,k}$-$D_{\text{Park-Ang}}$ relations.

$$D_{K,k} = f\left(\rho_{\text{sr}}, F_y, \Delta_y, \Delta_{k,\max}, \mu, m, T, A_g, V_g, t_d\right). \quad (16)$$

From equation (16), it can be seen that the stiffness decay index $D_{K,k}$ is effectively related to the structural parameters (ρ_{sr}, F_y, Δ_y, $\Delta_{k,\max}$, μ, m, and T) and seismic parameters (A_g, V_g, and t_d).

4.2. The Seismic Design Process Based on Stiffness Decay Index. According to equation (16), when the structural parameters (F_y, Δ_y, $\Delta_{k,\max}$, μ, m, and T) and seismic parameters (A_g, V_g, and t_d) are determined, the correspondence correlation between the stiffness decay index $D_{K,k}$ and the transverse reinforcement ratio ρ_{sr} is established. On this basis, the seismic design process based on stiffness decay index is proposed. The seismic design process includes the following six steps.

4.2.1. Determination of m and T. The sectional dimensions and material characteristics of the structure are initially selected, and the elastic response spectrum method is used to obtain the seismic effect [8]. Then, the seismic effect and gravity effect are combined to calculate the reinforcement of the structure. The mass m and lateral stiffness K can be calculated based on the sectional dimensions and material characteristics. The fundamental period T can be obtained by the following equation:

$$T = 2\pi\sqrt{\frac{m}{K}}. \quad (17)$$

4.2.2. Determination of μ and $\Delta_{k,max}$. The nonlinear analysis program (MIDAS Gen) is used to establish the SDOF structural model. Pushover analysis is performed on the

structural model, which can obtain the capacity curve of the structure and the demand spectrum curve for moderate earthquake action [28]. The intersection of capability curve and the demand spectrum curve is defined as the performance point for moderate earthquake action. The deformation value at the performance point is the maximum displacement of the structure, and it is also the maximum displacement $\Delta_{k,\max 1}$ of RC column components under moderate earthquake action. Based on the value of spectral deformation $S_{\max}$ at the performance point and the value of spectral deformation S_y at the yield point, the value of the ductility coefficient μ_1 for moderate earthquake action can be determined according to equation (18). Similarly, the maximum displacement $\Delta_{k,\max 2}$ of RC column components and the value of ductility coefficient μ_2 under major earthquake action can be obtained.

$$\mu = \frac{S_{\max}}{S_y}. \tag{18}$$

4.2.3. Determination of F_y and Δ_y. According to the sectional dimension and longitudinal reinforcement of RC column components, the yield displacement Δ_y of RC column components can be determined by performing push-over analysis [28]. Based on the yield displacement Δ_y, elastic modulus of concrete E, moment of inertia I, and height of column component, and the yield force F_y of RC column components can be determined by the following equation:

$$F_y = \frac{3EI}{H^3}\Delta_y. \tag{19}$$

4.2.4. Determination of V_g and A_g. The peak values of ground acceleration A_g under moderate and major earthquake in the seismic design code for buildings were proposed [8]. To obtain the peak values of ground velocity (V_g), the ratio of V_g to A_g is set at 0.15 s in the process of seismic design [28]. Table 3 shows the peak values of ground acceleration A_g for moderate and major earthquake.

4.2.5. Determination of t_d. From [24], it can be found that when the earthquake duration t_d lasts between 0 and 10 seconds, the damage of RC column components increases rapidly, when the earthquake duration t_d lasts between 10 and 20 seconds, the growth rate of damage slows down, when the earthquake duration t_d lasts between 20 and 30 seconds, the influence of earthquake duration on the damage gradually disappears. Therefore, the seismic duration t_{d} between 0 and 30 seconds can be considered.

4.2.6. Determination of ρ_{sr}. When the mass m, fundamental period T, ductility coefficient μ_1, maximum displacement amplitude $\Delta_{k,\max 1}$, yield load F_y, yield displacement Δ_y, peak value of ground acceleration A_g, peak value of ground velocity V_g, earthquake duration t_d, and performance design objectives (the stiffness degradation $D_{K,k}$) are determined, the transverse reinforcement ratio $\rho_{\mathrm{sr}1}$ for moderate earthquake can be determined. Similarly, the transverse reinforcement ratio $\rho_{\mathrm{sr}2}$ for major earthquake can be determined. Comparing the transverse reinforcement ratio $\rho_{\mathrm{sr}1}$ and $\rho_{\mathrm{sr}2}$, the larger value is chosen as the final transverse reinforcement ratio.

Table 3: The peak values of ground acceleration A_g for moderate and major earthquake [8].

Seismic intensity	Moderate earthquake (cm/s^2)	Major earthquake (cm/s^2)
6 degrees (0.05 g)	45	125
7 degrees (0.10 g)	98	220
7 degrees (0.15 g)	147	310
8 degrees (0.20 g)	196	400
8 degrees (0.30 g)	294	510
9 degrees (0.40 g)	392	620

4.3. Example. The design process is introduced according to the SDOF structure, and the relevant design conditions of the SDOF structure are shown in Table 4. Referring to Table 4, H is the height of the RC column components, L is the span of the RC beam components, b is the height of the cross-section, h is the width of the cross-section, HRB represents the type of longitudinal reinforcement, HPB represents the type of transverse reinforcement, and C represents the type of concrete. Figure 6 shows the SDOF structural model.

In this example, the site is set as Class II, the seismic intensity is set as 8 degrees (0.2 g), and the earthquake group is set as the first group. The floor load is set to 100 kN/m^2. The earthquake duration 2.5, 5, 10, 20, and 30 seconds are considered. Due to the same reinforcement of the RC column components, the column A is chosen as an example to introduce seismic design process. Table 5 is the calculated values of the structural parameters and seismic parameters. Figure 7 shows the correlation between the transverse reinforcement ratio and stiffness decay index under different earthquake duration conditions.

According to Figure 7, it can be found that when the stiffness decay index $D_{K,k}$ remains unchanged, the transverse reinforcement ratio ρ_{sr} increases continuously with the increase of earthquake duration. When the earthquake duration t_d lasts between 0 and 10 seconds, the transverse reinforcement ratio ρ_{sr} increases rapidly, when the earthquake duration t_d lasts between 10 and 30 seconds, the growth rate of the transverse reinforcement ratio ρ_{sr} slows down. This indicates that the damage of RC column components is exacerbated by an increase in earthquake duration, and this effect tends to be more pronounced at the beginning of the earthquake and then gradually decreases over time. When the earthquake duration remains unchanged, the stiffness decay index decreases continuously with the increases of the transverse reinforcement ratio. The smaller the stiffness decay index $D_{K,k}$, the more transverse reinforcement is required. This indicates that increasing the amount of transverse reinforcement can be an effective means of limiting the damage development of RC column components.

Table 4: The relevant design conditions of the SDOF structure.

Member	H (mm)	L (mm)	b (mm)	h (mm)	HRB	HPB	C
Beams	—	4000	200	350	HRB335	HPB300	C30
Columns	3000	—	400	4000	HRB335	HPB300	C30

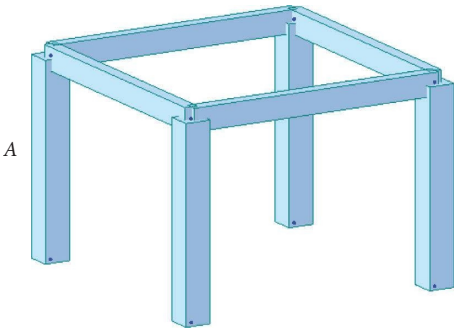

Figure 6: The SDOF structural model.

Table 5: The calculated values of the structural parameters and seismic parameters.

	m (kg)	T (s)	μ	$\Delta_{k,\max 1}$ (mm)	F_y (kN)	Δ_y (mm)	A_g (cm/s^2)	V_g (cm/s)
Moderate earthquakes	172547	0.49	1.46	13.17	64	9	196	29.4
Major earthquakes	172547	0.49	4.44	39.9	64	9	400	60

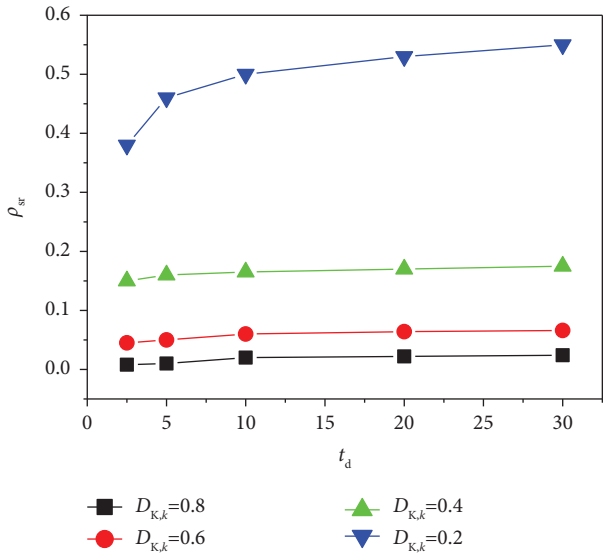

Figure 7: The correlation between the transverse reinforcement ratio and stiffness decay index under different earthquake duration conditions.

5. Conclusions

This design process is limited to RC square/rectangular column members for SDOF. The conclusions drawn in this paper are as follows.

(1) The design process based on stiffness decay index is proposed, which can compensate for the lack of considering the duration effect in current seismic design codes.

(2) The stiffness decay index is more suitable for defining structural damage compared to deformation index and Park-Ang index. The stiffness decay index establishes quantitative relationships with seismic parameters and structural parameters,

facilitating performance-based design in engineering practice.

(3) The increase in earthquake duration exacerbates the damage of RC column components, and this effect is more pronounced at the beginning of the earthquake and gradually decreases over time.

Data Availability

The data used to support the findings of this study are available from the corresponding author upon request.

Conflicts of Interest

The authors declare that they have no conflicts of interest.

Acknowledgments

This research was supported by the National Natural Science Foundation of China (Grant no. 52008159), Natural Science Foundation of Hunan Province (Grant no. 2022JJ40023), Scientific Research Project of Education Department of Hunan Province (Grant no. 20B108), and the Aid program for Science and Technology Innovative Research Team in Higher Educational Institutions of Hunan Province.

References

[1] J. Su, D. Wu, and X. Wang, "Influence of ground motion duration on seismic behavior of RC bridge piers: the role of low-cycle fatigue damage of reinforcing bars," *Engineering Structures*, vol. 279, Article ID 115587, 2023.

[2] P. Sun, C. Zhai, and W. Wen, "Experimental investigation on the damage accumulation of reinforced concrete columns under mainshock-aftershock sequences," *Earthquake Engineering and Structural Dynamics*, vol. 50, no. 15, pp. 4142–4160, 2021.

[3] N. A. Marafi, J. W. Berman, and M. O. Eberhard, "Ductility dependent intensity measure that accounts for ground motion spectral shape and duration," *Earthquake Engineering and Structural Dynamics*, vol. 45, no. 4, pp. 653–672, 2016.

[4] F. Ding, X. Wu, P. Xiang, and Z. Yu, "New damage ratio strength criterion for concrete and lightweight aggregate concrete," *ACI Structural Journal*, vol. 118, no. 6, pp. 165–178, 2021.

[5] J. Chen, C. Zhao, F. Ding, and P. Xiang, "Experimental study on the seismic behavior of precast concrete column with grouted corrugated sleeves and debonded longitudinal reinforcements," *Advances in Structural Engineering*, vol. 22, no. 15, pp. 3277–3289, 2019.

[6] A. Alothman, S. Mangalathu, A. Al-Mosawe, M. M. Alam, and A. Allawi, "The influence of earthquake characteristics on the seismic performance of reinforced concrete buildings in Australia with varying heights," *Journal of Building Engineering*, vol. 67, Article ID 105957, 2023.

[7] J. Chen, W. Wang, F. Ding et al., "Behavior of an advanced bolted shear connector in prefabricated steel-concrete composite beams," *Materials*, vol. 12, no. 18, p. 2958, 2019.

[8] GB 50011-2010, *Code for Seismic Design of Buildings: GB 50011-2010*, China Architecture and Building Press, Beijing, China, 2016.

[9] J. C. Goodnight, M. J. Kowalsky, and J. M. Nau, "Effect of load history on performance limit states of circular bridge columns," *Journal of Bridge Engineering*, vol. 18, no. 12, pp. 1383–1396, 2013.

[10] Y. Yang, Z. Liu, H. Tang, and J. Peng, "Deflection-based failure probability analysis of low shrinkage-creep concrete structures in presence of non-stationary evolution of shrinkage and creep uncertainties," *Construction and Building Materials*, vol. 376, Article ID 131077, 2023.

[11] Y. Feng, M. J. Kowalsky, and J. M. Nau, "Effect of seismic load history on deformation limit states for longitudinal bar buckling in RC circular columns," *Journal of Structural Engineering*, vol. 141, no. 8, Article ID 04014187, 2015.

[12] P. Xiang, Z. Deng, Y. Su, H. Wang, and Y. Wan, "Experimental investigation on joints between steel-reinforced concrete T-shaped column and reinforced concrete beam under bidirectional low-cyclic reversed loading," *Advances in Structural Engineering*, vol. 20, no. 3, pp. 446–460, 2017.

[13] A. Erberik and H. Sucuoğlu, "Seismic energy dissipation in deteriorating systems through low-cycle fatigue," *Earthquake Engineering and Structural Dynamics*, vol. 33, no. 1, pp. 49–67, 2004.

[14] H. Sucuoğlu and A. Erberik, "Energy-based hysteresis and damage models for deteriorating systems," *Earthquake Engineering and Structural Dynamics*, vol. 33, no. 1, pp. 69–88, 2004.

[15] Z. Liu, Y. Wang, H. Yuan, and K. Chen, "Damage evaluation of RC beams under variable amplitude loading histories," *Journal of Building Structures*, vol. 38, no. 11, pp. 132–141, 2017.

[16] Y. Yang, J. Peng, C. S. Cai, and H. Tang, "Probabilistic analysis of corrosion initiation in existing reinforced concrete structures with imprecise random field," *Structures*, Elsevier, vol. 52, pp. 877–888, 2023.

[17] S. K. Kunnath and Y. H. Chai, "Cumulative damage-based inelastic cyclic demand spectrum," *Earthquake Engineering and Structural Dynamics*, vol. 33, no. 4, pp. 499–520, 2004.

[18] Y. L. Mo and S. J. Wang, "Seismic behavior of RC columns with various tie configurations," *Journal of Structural Engineering*, vol. 126, no. 10, pp. 1122–1130, 2000.

[19] K. Poljanšek, I. Peruš, and P. Fajfar, "Hysteretic energy dissipation capacity and the cyclic to monotonic drift ratio for rectangular RC columns in flexure," *Earthquake Engineering and Structural Dynamics*, vol. 38, no. 7, pp. 907–928, 2009.

[20] J. Yuan and Y. Wang, "The influence of load histories to characteristic of energy dissipation and failure of prestressed concrete beams," *Engineering Mechanics*, vol. 24, no. 10, pp. 137–143, 2007.

[21] Y. Jiao, S. Yamada, S. Kishiki, and Y. Shimada, "Evaluation of plastic energy dissipation capacity of steel beams suffering ductile fracture under various loading histories," *Earthquake Engineering and Structural Dynamics*, vol. 40, no. 14, pp. 1553–1570, 2011.

[22] Z. Liu, Y. Wang, Z. Cao, Y. Chen, and Y. Hu, "Seismic energy dissipation under variable amplitude loading for rectangular RC members in flexure," *Earthquake Engineering and Structural Dynamics*, vol. 47, no. 4, pp. 831–853, 2018.

[23] Y. Wang, Z. Liu, W. Yang, Y. Hu, and Y. Chen, "Damage index of reinforced concrete members based on the energy dissipation capability degradation," *The Structural Design of Tall and Special Buildings*, vol. 29, no. 2, p. e1695, 2020.

[24] Z. F. Liu, Y. K. Wang, Z. X. Cao, and Y. Chen, "Study on performance index of RC members considering effect of

seismic duration," *Journal of Building Structures*, vol. 39, pp. 168–177, 2018.

[25] Y. J. Park and A. H. S. Ang, "Mechanistic seismic damage model for reinforced concrete," *Journal of Structural Engineering*, vol. 111, no. 4, pp. 722–739, 1985.

[26] Y. J. Park, A. H. S. Ang, and Y. K. Wen, "Seismic damage analysis of reinforced concrete buildings," *Journal of Structural Engineering*, vol. 111, no. 4, pp. 740–757, 1985.

[27] Y. H. Chai, P. Fajfar, and K. M. Romstad, "Formulation of duration-dependent inelastic seismic design spectrum," *Journal of Structural Engineering*, vol. 124, no. 8, pp. 913–921, 1998.

[28] Y. Wang, Z. Liu, D. Zhang, Z. Hu, and D. Yu, "Seismic design of rectangular/square columns in SDOF systems based on their damage performance," *Science Progress*, vol. 105, no. 4, Article ID 00368504221127788, 2022.